US Army Corps of Engineers
Hydrologic Engineering Center

A Finite Difference Method for Analyzing Liquid Flow in Variably Saturated Porous Media

April 1970

TP-22

REPORT DOCUMENTATION PAGE

Form Approved OMB No. 0704-0188

1. REPORT DATE *(DD-MM-YYYY)*	2. REPORT TYPE	3. DATES COVERED *(From - To)*
April 1970	Technical Paper	

4. TITLE AND SUBTITLE
A Finite Difference Method for Analyzing Liquid Flow in Variable Saturated Porous Media

5a. CONTRACT NUMBER

5b. GRANT NUMBER

5c. PROGRAM ELEMENT NUMBER

6. AUTHOR(S)
Richard L. Cooley

5d. PROJECT NUMBER

5e. TASK NUMBER

5F. WORK UNIT NUMBER

7. PERFORMING ORGANIZATION NAME(S) AND ADDRESS(ES)
US Army Corps of Engineers
Institute for Water Resources
Hydrologic Engineering Center (HEC)
609 Second Street
Davis, CA 95616-4687

8. PERFORMING ORGANIZATION REPORT NUMBER
TP-22

9. SPONSORING/MONITORING AGENCY NAME(S) AND ADDRESS(ES)

10. SPONSOR/ MONITOR'S ACRONYM(S)

11. SPONSOR/ MONITOR'S REPORT NUMBER(S)

12. DISTRIBUTION / AVAILABILITY STATEMENT
Approved for public release; distribution is unlimited.

13. SUPPLEMENTARY NOTES
Presented at the 51st Annual Meeting of the American Geophysical Union, Washington, DC, 20-24 April 1970.

14. ABSTRACT
Finite difference equations were derived by converting the original non-linear partial differential equation to an integral equation using the divergence theorem and integrating around individual mesh volumes. Application of the technique to the problem of axi-symmetric flow to a water well partially or completely penetrating an elastic unconfined aquifer demonstrates the use of the technique. Three methods were used to solve the matrix equations resulting from the scheme: a form of the direct alternating direction implicit method (ADIP), the iterative alternating direction implicit method (ADIPIT), and line successive over-relaxation (SLOR). The fastest method for the problems investigated so far was SLOR. The number of iterations required for SLOR and ADIPIT were similar, but ADIPIT requires two mesh sweeps per iteration. Excessively small time steps were required for convergence of ADIP. Original non-linearity of the differential equation was preserved by keeping saturations and relative permeabilities current with hydraulic heads in the iteration sequence, the averaging them over time. The mesh integration method appears to be well suited for application to regions having internal boundaries between sub-regions of different rock properties because it directly utilizes the boundary conditions acting at the interfaces.

15. SUBJECT TERMS
groundwater movement, porous media, model studies, saturated flow, hydraulic conductivity, porosity, transmissivity, aquifer characteristics, hydrogeology, mathematical models, equations, viscosity, water table, rock properties, analytical techniques, methodology

16. SECURITY CLASSIFICATION OF: a. REPORT	b. ABSTRACT	c. THIS PAGE	17. LIMITATION OF ABSTRACT	18. NUMBER OF PAGES	19a. NAME OF RESPONSIBLE PERSON
U	U	U	UU	52	19b. TELEPHONE NUMBER

Standard Form 298 (Rev. 8/98)
Prescribed by ANSI Std. Z39-18

A Finite Difference Method for Analyzing Liquid Flow in Variably Saturated Porous Media

April 1970

US Army Corps of Engineers
Institute for Water Resources
Hydrologic Engineering Center
609 Second Street
Davis, CA 95616

(530) 756-1104
(530) 756-8250 FAX
www.hec.usace.army.mil

TP-22

INTRODUCTION

In recent years a number of workers have stressed the necessity of a unified approach to the study of subsurface water flow above and below the water table because from a fluid dynamic point of view the water table is an artificial boundary (Stallman, 1961, p. 40, Childs, 1960, p. 781, Freeze, 1969, p. 153, Klute, 1969, pp. 61-62). In connection with this general concept, it is of particular importance to include phenomena taking place in the unsaturated region when analyzing unconfined ground water flow problems (Taylor and Luthin, 1969, p. 144, Rubin, 1968, p. 607, Cooley and Donohue, 1969, p. 2). As has been pointed out in the above mentioned references, solutions to unconfined flow problems have often been unrealistic because, among other simplifications, the water table was treated as a fluid discontinuity across which only a known quantity of fluid could move (e.g., when using the Dupuit-Forchheimer assumptions or the concept of a classical bounding surface (Lamb, 1945, pp. 6-8)). However, the water table is generally not a discontinuity, and replenishment to the saturated region from the unsaturated zone (and vice versa) is usually a consequence of water movement in the unsaturated zone, even for steady-state flow (see for instance Taylor and Luthin, 1961, p. 151, figure 4). In order to study subsurface water flow under variably saturated conditions and verify the use of the theory under field conditions, satisfactory methods of solving the nonlinear partial differential equations governing flow for general problems must be developed.

Flow of water in unsaturated regions is generally treated as a special case of multiphase fluid flow whereby the movement of one phase, air, is neglected. Unsteady-state, multiphase fluid flow has been investigated by a number of workers in the petroleum industry (see for example, Douglas, Peaceman, and Rachford, 1959, Welge and Weber, 1964, Fagin and Stewart, 1966, Coats, Nielsen, Terhune, and Weber, 1967, Breitenbach, Thurnau, and van Poolen, 1968a, Breitenbach, Thurnau, and van Poolen, 1968b, and Breitenbach, Thurnau, and van Poolen, 1968c). The solution methods developed for these multiphase flow problems provide valuable background for development of solutions to problems of water flow in variably saturated porous media.

One problem in the general class discussed above is flow to a well being pumped in an unconfined flow system. Taylor and Luthin (1969) have outlined a finite difference procedure that involves explicit extrapolation of the water table position and water content distribution in the unsaturated region and implicit solution for head distribution in the saturated region for each time step. They have applied the method to a well that fully penetrates a single incompressible aquifer. The objectives of the study reported herein are (1) to develop an implicit finite difference solution to the problem of axi-symmetric flow to a water well that partially or completely penetrates one or more horizontal elastic rock units, the upper one of which is unconfined, and (2) to design the method to be potentially applicable to other problems of liquid flow in variably saturated porous media. This report is an extension of previous work by Cooley and Donohue (1969).

MATHEMATICAL FORMULATION OF PROBLEM

All symbols used are defined in the "Notation" section of the appendix. The indices are defined separately at the end of that section.

For the purposes of the present study, the variably saturated porous medium is assumed to deform elastically in response to fluid pressure changes similarly to the manner of completely saturated elastic porous material. Thus, application of the following development is restricted to cases involving water saturation greater than residual water saturation. When water saturation equals residual water saturation, water is assumed to be immobile. Using the concept of coordinates deforming because of elastic compression or expansion of the porous medium (Cooper, 1966), the continuity equation is

$$-\iiint_{V(t)} \nabla\cdot(\rho\vec{v})dV = \frac{\partial}{\partial t}\iiint_{V(t)} S_w \rho n dV. \tag{1}$$

In the volume element $V(t) = \Delta x\Delta y\Delta z$, Δz is taken as the deforming coordinate. Equation 1 can be expanded and rearranged (see appendix) to yield

$$\iiint_{V(t)} \left[\nabla\cdot(\rho\vec{v})+\rho n\,\frac{\partial S_w}{\partial t} + S_w\left(n\,\frac{\partial \rho}{\partial t} + \rho\,\frac{\partial n}{\partial t} + \rho n\,\frac{\partial w_g}{\partial z}\right)\right] dV=0. \tag{2}$$

Because this equation must hold for any arbitrary volume,

$$-\nabla\cdot(\rho\vec{v}) = \rho n\,\frac{\partial S_w}{\partial t} + S_w\left(n\,\frac{\partial \rho}{\partial t} + \rho\,\frac{\partial n}{\partial t} + \rho n\,\frac{\partial w_g}{\partial z}\right). \tag{3}$$

The term in parentheses in equation 3 can be approximated for small changes in fluid density, ρ, as $\rho S_s\,\frac{\partial H}{\partial t}$ (see appendix or Cooper, 1966, pp. 4788-4789) where

$$S_s = n\rho g(c+c_n). \tag{4}$$

Change in fluid density with pressure is very small. Cooper (1966, p. 4789) has stated that the term resulting from assuming ρ variable in $\nabla\cdot(\rho\vec{v})$ is usually negligible. Using the relationship for S_s and $\nabla\cdot(\rho\vec{v})\simeq\rho\nabla\cdot\vec{v}$, equation 3 becomes

$$-\nabla\cdot\vec{v} = n\,\frac{\partial S_w}{\partial t} + S_w S_s\,\frac{\partial H}{\partial t}\,. \tag{5}$$

One form of Darcy's law for water partially or completely saturating a porous medium is

$$\vec{v} = -\,KK_r\nabla H. \tag{6}$$

Combining equations 5 and 6 there results

$$\nabla\cdot(KK_r\nabla H) = n\,\frac{\partial S_w}{\partial t} + S_w S_s\,\frac{\partial H}{\partial t}\,. \tag{7}$$

The first term on the right side of equation 7 can be modified using the definition of air saturation ($S_a = 1-S_w$) and capillary pressure ($P_c=P_a-P$), and the assumption that they are related uniquely for either imbibition or drainage (Douglas, Peaceman, Rachford, 1959, p. 298):

$$n\,\frac{\partial S_w}{\partial t} = n\,\frac{dS_w}{dP_c}\,\frac{\partial P_c}{\partial t} = -n\,\frac{dS_a}{dP_c}\left(\frac{\partial P_a}{\partial t} - \frac{\partial P}{\partial t}\right). \tag{8}$$

If it is assumed that the change in air pressure, P_a, will be much smaller than the change in water pressure, P, with time

$$-n\,\frac{dS_a}{dP_c}\,\frac{\partial P_c}{\partial t} \simeq -n\,\frac{dS_a}{dP}\,\frac{\partial P}{\partial t} \simeq -n\rho g\,\frac{dS_a}{dP}\,\frac{\partial H}{\partial t}\,. \tag{9}$$

Equation 7 may therefore be written

$$\nabla\cdot(KK_r\nabla H) = \left(S_w S_s - n\rho g\,\frac{dS_a}{dP}\right)\frac{\partial H}{\partial t}\,. \tag{10}$$

In the present study hydraulic properties are considered to be constant in any one rock unit, ir, but to vary between units. The equation for each unit written in the cylindrical coordinate system with axial symmetry is

$$\frac{1}{R}\frac{\partial}{\partial R}\left(K_r R \frac{\partial H}{\partial R}\right) + \frac{\partial}{\partial Z}\left(K_r \frac{\partial H}{\partial Z}\right) = \left(\frac{S_w (S_s)_{ir}}{K_{ir}} - \frac{n_{ir}\rho g}{K_{ir}}\frac{dS_a}{dP}\right)\frac{\partial H}{\partial t} \qquad (11)$$

In order for one solution to apply to a number of different problems, equation 11 should be rewritten in dimensionless form (Smith, 1965, p. 9). For the dimensionless variables defined in the appendix, equation 11 becomes

$$\frac{1}{r}\frac{\partial}{\partial r}\left(K_r r \frac{\partial h}{\partial r}\right) + \frac{\partial}{\partial z}\left(K_r \frac{\partial h}{\partial z}\right) = \left(S_w (S_r)_{ir} - \frac{dS_a^D}{dp_h}\right)\frac{(S_y)_{ir}^D}{K_{ir}^D}\frac{\partial h}{\partial t^D} \qquad (12)$$

Boundary conditions used for the problem, illustrated in figure 1, are similar to those used by Taylor and Luthin (1969) and Rubin (1968) for similar problems. Using dimensionless variables, at the well bore, r_w,

$$\left.\begin{array}{lll} \dfrac{\partial h}{\partial r} = 0 & 0 \le z \le z_B & t^D \ge 0 \\ h = h_w & z_B \le z \le h_w & t^D \ge 0 \\ h = z & h_w \le z \le z_s & t^D \ge 0 \\ \dfrac{\partial h}{\partial r} = 0 & z_s \le z \le b_T & t^D \ge 0 \end{array}\right\} \qquad (13)$$

The hydraulic head in the well bore, h_w, is to be interpreted as the value necessary to yield a prescribed constant discharge, Q. On the top and bottom boundaries (i.e., at $z = b_T$ and $z = 0$, respectively)

$$\frac{\partial h}{\partial z} = 0 \qquad r_w \le r \le r_e \qquad t^D \ge 0 \qquad (14)$$

At the lateral external boundary, r_e,

$$h = h_e \qquad 0 \le z \le b_T \qquad t^D \ge 0 \qquad (15)$$

The boundary conditions at the horizontal interfaces between rock units are

$$(KK_r \frac{\partial h}{\partial z})_{ir} = (KK_r \frac{\partial h}{\partial z})_{ir+1} \qquad (16)$$

and

$$(\frac{\partial h}{\partial r})_{ir} = (\frac{\partial h}{\partial r})_{ir+1} \qquad (17)$$

The initial condition

$$h = h_e \qquad r_w \le r \le r_e \qquad 0 \le z \le b_T \qquad t^D = 0 \qquad (18)$$

completes the basic formulation of the problem.

In addition to the basic differential equation and its boundary and initial conditions, relationships between water pressure, relative permeability, and saturation must be stated. **The following functions are used in this study because of their usefulness for expressing a wide variety of conditions:**

$$S_a^D = \frac{(-p_h)^c}{(-p_h)^c + A}, \qquad p_h \le 0 \qquad (19)$$

and

$$K_r = \left[\frac{S_{ar} - S_a}{S_{ar}} \right]^d = (1 - S_a^D)^d, \qquad S_a \le S_{ar} \qquad (20)$$

Equation 20 is a generalization of an equation given by Corey (1954, p. 39).

FINITE DIFFERENCE EQUATIONS

Finite difference equations were derived using the mesh integration method of Varga (Varga, 1962, pp. 182-186, 190-191, Spanier, 1967, pp. 219-222) generalized to retain, in an approximate manner, the nonlinear aspects of equation 12. To use the method the entire region being analyzed is divided into a rectangular mesh, each internal node point of which is enclosed by a mesh volume (figure 2). Boundaries of the volume element extend to half the distance between the central and all adjacent node points for all interior nodes. Because the mesh is arranged so that node points lie on rock-property region and external boundaries, a region boundary divides mesh volumes lying along it in half, and only one half of a mesh volume exists on external boundaries (figure 2).

Neglecting the small change in volume of mesh volume element V_ℓ due to elastic deformation, equation 12 can be restated in integral form for a volume element internal to a rock property region or external boundary using the divergence theorem:

$$K_{ir}^{D} \iiint\limits_{V_\ell} \left[\frac{1}{r}\frac{\partial}{\partial r}\left(K_r r \frac{\partial h}{\partial r}\right) + \frac{\partial}{\partial z}\left(K_r \frac{\partial h}{\partial z}\right)\right] dV = K_{ir}^{D} \iint\limits_{S_\ell} K_r \frac{\partial h}{\partial N}\, dS$$

$$= (S_y)_{ir}^{D} \iiint\limits_{V_\ell} \left[S_w (S_r)_{ir} - \frac{dS_a^D}{dp_h}\right] \frac{\partial h}{\partial t^D}\, dV \qquad (21)$$

where N is the direction normal to surface S_ℓ enclosing volume element V_ℓ. For a volume element lying on a rock property region boundary,

$$K_{ir}^{D} \iint\limits_{(S_\ell)_{ir}} K_r \frac{\partial h}{\partial N}\, dS + K_{ir+1}^{D} \iint\limits_{(S_\ell)_{ir+1}} K_r \frac{\partial h}{\partial N}\, dS$$

$$=(S_y)^D_{ir} \iiint\limits_{(V_\ell)_{ir}} \left[S_w (S_r)_{ir} - \frac{dS^D_a}{dp_h}\right] \frac{\partial h}{\partial t^D}\, dV$$

$$+(S_y)^D_{ir+1} \iiint\limits_{(V_\ell)_{ir+1}} \left[S_w (S_r)_{ir+1} - \frac{dS^D_a}{dp_h}\right] \frac{\partial h}{\partial t^D}\, dV \tag{22}$$

The symbol $(S_\ell)_{ir}$ refers to the half of the surface lying in region ir, and the other symbols involving S_ℓ and V_ℓ are to be interpreted similarly. It should be noted that the **portions of the surface integrals expressing discharge** across the boundary are of equal value but opposite sign, thus cancelling one another.

Equation 21 can be rewritten in the (r,z) coordinate system yielding

$$2\pi r_{i+1/2}\, K^D_{ir} \int_{z_{j-1/2}}^{z_{j+1/2}} K_r \frac{\partial h}{\partial r}\, dz - 2\pi r_{i-1/2} K^D_{ir} \int_{z_{j-1/2}}^{z_{j+1/2}} K_r \frac{\partial h}{\partial r}\, dz$$

$$+2\pi K^D_{ir} \int_{r_{i-1/2}}^{r_{i+1/2}} K_r \frac{\partial h}{\partial z}\, rdr \Bigg|_{z=z_{j+1/2}} - 2\pi K^D_{ir} \int_{r_{i-1/2}}^{r_{i+1/2}} K_r \frac{\partial h}{\partial z}\, rdr \Bigg|_{z=z_{j-1/2}}$$

$$=2\pi (S_y)^D_{ir} \int_{z_{j-1/2}}^{z_{j+1/2}} \int_{r_{i-1/2}}^{r_{i+1/2}} \left[S_w (S_r)_{ir} - \frac{dS^D_a}{dp_h}\right] \frac{\partial h}{\partial t^D}\, rdrdz \tag{23}$$

Equation 22 gives a similar equation except the right side and the first and second terms on the left side of equation 23 are each split into two integrals, one for each region, with limits to the integrals in the z direction extending from z_j to $z_{j+1/2}$ and from $z_{j-1/2}$ to z_j.

Each of the integrals on the left side of equation 23 is now approximated by terms of the form

$$2\pi r_{i+1/2}K^D_{ir}\int_{z_{j-1/2}}^{z_{j+1/2}} K_r \frac{\partial h}{\partial r}\,dz \simeq 2\pi r_{i+1/2}K^D_{ir}(K_r)_{i+1/2,j}\left(\frac{h_{i+1,j}-h_{i,j}}{r_{i+1}-r_i}\right)\int_{z_{j-1/2}}^{z_{j+1/2}} dz$$

$$=(K_rA_x)_{i+1/2,j}\;(h_{i+1,j}-h_{i,j}) \tag{24}$$

The right side of equation 23 takes the form

$$2\pi (S_y)^D_{ir}\int_{z_{j-1/2}}^{z_{j+1/2}}\int_{r_{i-1/2}}^{r_{i+1/2}}\left[S_w(S_r)_{ir}-\frac{dS^D_a}{dp_h}\right]\frac{\partial h}{\partial t^D}\;rdrdz$$

$$\simeq 2\pi (S_y)^D_{ir}\left[(S_w)^{(n+1/2)}_{i,j}(S_r)_{ir}-\left(\frac{\Delta S^D_a}{\Delta p_h}\right)^{(n+1/2)}_{i,j}\right]\frac{h^{(n+1)}_{i,j}-h^{(n)}_{i,j}}{\Delta t^D}\int_{z_{j-1/2}}^{z_{j+1/2}}\int_{r_{i-1/2}}^{r_{i+1/2}} rdrdz$$

$$=\frac{(V_b)_{i,j}}{\Delta t^D}\left[(S_w)^{(n+1/2)}_{i,j}(S_r)_{ir}-\left(\frac{\Delta S^D_a}{\Delta p_h}\right)^{(n+1/2)}_{i,j}\right](h^{(n+1)}_{i,j}-h^{(n)}_{i,j}) \tag{25}$$

where

$$\left(\frac{\Delta S^D_a}{\Delta p_h}\right)^{(n+1/2)}_{i,j}=\frac{(S^D_a)^{(n+1)}_{i,j}-(S^D_a)^{(n)}_{i,j}}{(p_h)^{(n+1)}_{i,j}-(p_h)^{(n)}_{i,j}}$$

and

$$(S_w)^{(n+1/2)}_{i,j}=\frac{1}{2}\left[(S_w)^{(n+1)}_{i,j}+(S_w)^{(n)}_{i,j}\right].$$

Equation 24 and the other similar terms must be placed somewhere in the time interval n, n+1. Because the actual placement depends on the method used to solve the finite difference equations, discussion will be deferred until the solution methods are explained.

It is important to note that, because node points are placed on internal boundaries, dual values of K_r and S_a^D will exist at these points. One value is calculated using equations 19 and 20 with constants A, c, and d characteristic of one region, and one value is calculated using constants characteristic of the other region. Each value of K_r and S_a^D is used with its appropriate integral term.

On all external boundaries the finite difference equations must be modified to incorporate the boundary conditions. Where the head, h, is known on the boundary, this is accomplished by using the known head in its appropriate place in equations written for node points just interior to the boundary. Equations are not written for boundary points. For the no flow boundaries the node point on the boundary is unknown, and a reflection condition is imposed using an imaginary line of points just outside the boundary. For example, at the well bore,

$$\frac{\partial h}{\partial r} \simeq \frac{h_{2,j} - h_{o,j}}{r_2 - r_o} = 0, \qquad (26)$$

where i = 1 at the well bore, and equation 24 would become

$$2\pi r_1 K_{ir}^D \int_{z_{j-1/2}}^{z_{j+1/2}} K_r \frac{\partial h}{\partial r} dz \simeq (K_r A_x)_{1,j} \; (h_{2,j} - h_{o,j}) = 0 \qquad (27)$$

Therefore, the reflection condition is imposed simply by eliminating the term for discharge across the boundary from each boundary point equation where the no flow condition exists.

SOLUTION METHODS

Three methods were selected to solve the matrix equations resulting from the finite difference scheme: a form of the direct alternating direction implicit method (ADIP), the iterative alternating direction implicit method (ADIPIT), and line successive over-relaxation (SLOR). The first two methods have only been applied to problems involving wells that fully penetrate a single, elastic, unconfined aquifer; whereas, the third has been applied to more general problems.

The ADIP applied to time level (n+1/2) involves replacing difference approximations for flow in one direction (for instance, the r direction) by an implicit approximation (Smith, 1965, pp. 17-18) and replacing the derivatives for flow in the other direction (i.e., the z direction) by an explicit formulation (Smith, 1965, p. 11). At the time level (n+1) the derivatives approximated by the implicit and explicit methods are reversed. This two-step procedure is then repeated to advance to time step (n+2), etc., through all time steps. For an implicit solution in the r direction the finite difference equation for nodes interior to a boundary are

$$(K_r A_x)^{(n+1/2)}_{i+1/2,j}\,(h_{i+1,j} - h_{i,j})^{(n+1/2)} - (K_r A_x)^{(n+1/2)}_{i-1/2,j}(h_{i,j} - h_{i-1,j})^{(n+1/2)}$$

$$+(K_r A_x)^{(n)}_{i,j+1/2}(h_{i,j+1} - h_{i,j})^{(n)} - (K_r A_z)^{(n)}_{i,j-1/2}(h_{i,j} - h_{i,j-1})^{(n)}$$

$$= \frac{(V_b)_{i,j}}{\Delta t^D/2} \left[(S_w)_{i,j}^{(n+1/2)} (S_r)_{ir} - \left(\frac{\Delta S_a^D}{\Delta p_h} \right)_{i,j}^{(n+1/4)} \right] (h_{i,j}^{(n+1/2)} - h_{i,j}^{(n)}) \qquad (28)$$

and, for implicit solution in the z direction,

$$(K_r A_x)_{i+1/2,j}^{(n+1/2)} (h_{i+1,j} - h_{i,j})^{(n+1/2)} - (K_r A_x)_{i-1/2,j}^{(n+1/2)} (h_{i,j} - h_{i-1,j})^{(n+1/2)}$$

$$+(K_r A_z)_{i,j+1/2}^{(n+1)} (h_{i,j+1} - h_{i,j})^{(n+1)} - (K_r A_z)_{i,j-1/2}^{(n+1)} (h_{i,j} - h_{i,j-1})^{(n+1)}$$

$$= \frac{(V_b)_{i,j}}{\Delta t^D/2} \left[(S_w)_{i,j}^{(n+1/2)} (S_r)_{ir} - \left(\frac{\Delta S_a^D}{\Delta p_h} \right)_{i,j}^{(n+3/4)} \right] (h_{i,j}^{(n+1)} - h_{i,j}^{(n+1/2)}) \qquad (29)$$

where

$$\left(\frac{\Delta S_a^D}{\Delta p_h} \right)_{i,j}^{(n+1/4)} = \frac{(S_a^D)_{i,j}^{(n+1/2)} - (S_a^D)_{i,j}^{(n)}}{(p_h)_{i,j}^{(n+1/2)} - (p_h)_{i,j}^{(n)}}$$

and the corresponding term in equation 29 is defined **in a similar manner. Equations for node points on no flow boundaries have one complete term deleted as indicated by equation 27.**

If each of the four terms on the left sides of equations 28 and 29 are replaced with Q's for simplicity and then the equations are added, there results

$$(Q_{i+1/2,j}^{(n+1/2)} - Q_{i-1/2,j}^{(n+1/2)}) + \frac{1}{2} \left[(Q_{i,j+1/2}^{(n)} + Q_{i,j+1/2}^{(n+1)}) - (Q_{i,j-1/2}^{(n)} + Q_{i,j-1/2}^{(n+1)}) \right]$$

$$= \frac{(V_b)_{i,j}}{\Delta t^D} \left[(S_w)_{i,j}^{(n+1/2)} (S_r)_{ir} (h_{i,j}^{(n+1)} - h_{i,j}^{(n)}) - (S_a^D)_{i,j}^{(n+1)} + (S_a^D)_{i,j}^{(n)} \right] \qquad (30)$$

This equation, which is approximately centered in the time interval n,n+1, is analogous (except for the dependence of S_a^D and K_r on values of p_h) to the unsteady-state heat flow equation solved by ADIP given by Spanier (1967, p. 235, equation 58).

The method as defined by equations 28 and 29 cannot be applied directly because S_a^D and K_r are not known initially. A successive approximation or iteration technique was used in order to make S_a^D and K_r at each node agree with the value of p_h at the node. Values obtained at the last time level (for instance n) were used initially, the appropriate equation (for instance, equation 28) was solved, then S_a^D was recalculated from the new head. The new S_a^D for use with the next approximation was obtained from

$$(S_a^D)_{i,j}^{(k)} = (S_a^D)_{i,j}^{(k-1)} + \omega_s \left[(\hat{S}_a^D)_{i,j}^{(k)} - (S_a^D)_{i,j}^{(k-1)} \right], \qquad o \le \omega_s \le 1 \tag{31}$$

where $(S_a^D)_{i,j}^{(k-1)}$ is the value computed from the (k-1)th approximation, $(\hat{S}_a^D)_{i,j}^{(k)}$ is the value computed from the kth approximation (i.e., the value just computed from pressure head $(p_h)_{i,j}$), and $(S_a^D)_{i,j}^{(k)}$ is the interpolated value to be used for the next approximation. This procedure was necessary because, if $(\hat{S}_a^D)_{i,j}^{(k)}$ was used directly in the next iteration, the method frequently diverged. The value of $(K_r^{(k)})_{i,j}$ was calculated from $(S_a^D)_{i,j}^{(k)}$. Iterations were stopped when

$$|h_{i,j}^{(k+1)} - h_{i,j}^{(k)}| \quad \le 10^{-6},$$

and convergence was always obtained within 5 to 10 iterations.

After convergence, if the discharge yielded by h_w was correct, advancement was made to the next time level (for instance, (n+1/2)), and the iterative method was applied to the appropriate equation (equation 29 for the examples used above). The procedure for finding h_w to yield the correct discharge is discussed further on.

The ADIPIT is similar to ADIP except directions for implicit and explicit solutions are alternated during iterations at time step (n+1). Equations for the method at an internal node point are

$$
\begin{aligned}
&(K_rA_x)^{(k,n+1/2)}_{i+1/2,j}(h_{i+1,j}-h_{i,j})^{(k+1/2,n+1)}-(K_rA_x)^{(k,n+1/2)}_{i+1/2,j}(h_{i,j}-h_{i-1,j})^{(k+1/2,n+1)}\\
&+(K_rA_z)^{(k,n+1/2)}(h_{i,j+1}-h_{i,j})^{(k,n+1)}-(K_rA_z)^{(k,n+1/2)}(h_{i,j}-h_{i,j-1})^{(k,n+1)}\\
&=\frac{(V_b)_{i,j}}{\Delta t^D}\left[(S_w)^{(k,n+1/2)}_{i,j}(S_r)_{ir}-\left(\frac{\Delta S_a^D}{\Delta p_h}\right)^{(k,n+1/2)}_{i,j}\right](h^{(k+1/2,n+1)}_{i,j}-h^{(n)}_{i,j})\\
&+\omega_{k+1/2}\left[\overline{(K_rA)}^{(k,n+1/2)}_{i,j}\right](h^{(k+1/2,n+1)}_{i,j}-h^{(k,n+1)}_{i,j})
\end{aligned}
\tag{32}
$$

and

$$
\begin{aligned}
&(K_rA_x)^{(k,n+1/2)}_{i+1/2,j}(h_{i+1,j}-h_{i,j})^{(k+1/2,n+1)}-(K_rA_x)^{(k,n+1/2)}_{i+1/2,j}(h_{i,j}-h_{i-1,j})^{(k+1/2,n+1)}\\
&+(K_rA_z)^{(k,n+1/2)}(h_{i,j+1}-h_{i,j})^{(k+1,n+1)}-(K_rA_z)^{(k,n+1/2)}(h_{i,j}-h_{i,j-1})^{(k+1,n+1)}\\
&=\frac{(V_b)_{i,j}}{\Delta t^D}\left[(S_w)^{(k,n+1/2)}_{i,j}(S_r)_{ir}-\left(\frac{\Delta S_a^D}{\Delta p_h}\right)^{(k,n+1/2)}_{i,j}\right](h^{(k+1,n+1)}_{i,j}-h^{(n)}_{i,j})\\
&+\omega_{k+1/2}\left[\overline{(K_rA)}^{(k,n+1/2)}_{i,j}\right](h^{(k+1,n+1)}_{i,j}-h^{(k+1/2,n+1)}_{i,j})
\end{aligned}
\tag{33}
$$

where

$$(K_rA_x)^{(k,n+1/2)}_{i+1/2,j} = \frac{1}{2} \left[(K_rA_x)^{(k,n+1)}_{i+1/2,j} + (K_rA_x)^{(n)}_{i+1/2,j} \right]$$

etc. for similar terms,

$$\overline{(K_rA)}_{i,j} = (K_rA_x)_{i+1/2,j} + (K_rA_x)_{i-1/2,j} + (K_rA_z)_{i,j+1/2} + (K_rA_z)_{i,j-1/2}$$

and

$$\left(\frac{\Delta S^D_a}{\Delta p_h}\right)^{(k,n+1/2)}_{i,j} = \frac{(S^D_a)^{(k,n+1)}_{i,j} - (S^D_a)^{(n)}_{i,j}}{(p_h)^{(k,n+1)}_{i,j} - (p_h)^{(n)}_{i,j}}$$

Equations 32 and 33 can be envisioned as relationships for iteration through "pseudo time" at each real time step. The last term of each equation is analogous to the storage change term in equations 28 and 29 with the acceleration parameter, $\omega_{k+1/2}$, occupying the position of $2/\Delta t^D$ and $\overline{(K_rA)}^{(k,n+1)}_{i,j}$, called a normalizing matrix, being used to accelerate convergence (Douglas, Peaceman, and Rachford, 1959, p. 307, and Douglas, 1962, p. 62). The form of the normalizing matrix used here is that of Welge and Weber (1964, p. 352-353). Convergence of the process at time step (n+1) has been reached when "pseudo steady-state" conditions occur, that is, whenever

$$\left| h^{(k+1)}_{i,j} - h^{(k)}_{i,j} \right|^{(n+1)} \leq \varepsilon$$

where ε is some small number (chosen as 10^{-7} in this study).

Speed of convergence depends greatly on the choice of $\omega_{k+1/2}$. For the case involving linear difference equations it can be shown that a sequence of parameters, in which each value is changed either at each half iteration (at k+1/2, k+1, k+3/2, etc) or at the end of each complete iteration, produces the most rapid convergence. Usually the sequence starts with the largest value, then each parameter is used in decreasing order of magnitude until the minimum is reached. At this point the cycle is restarted using the largest value again, and the process is continued until convergence results. The maximum and minimum values can be shown to be the maximum and minimum eigenvalues of the tridiagonal matrices resulting from the difference approximations for flow in the r or z directions if these tridiagonal matrices commute. Also, if these matrices commute and are nonnegative definite, the optimum number and value of the parameters $\omega_{max} \geq \omega_{k+1/2} \geq \omega_{min}$ can be calculated. An excellent review of the theory and procedures developed can be found in Spanier (1967). For the linear case involving noncommutating positive definite matrices, convergence is assured if enough acceleration parameters applied in monotonically nonincreasing order are used (Pearcy, 1962).

The procedures developed for the linear, commutative case have been used in the past (see for instance Douglas, Peaceman, and Rachford, 1959, Welge and Weber, 1964, and Coats, Nielsen, Terhune, and Weber, 1967) with good results, and this procedure has been adopted here. For equations 32 and 33, the maximum possible eigenvalue of linearized versions of either tridiagonal matrix is about 2.00, and, because convergence was found to be relatively insensitive to the value of the maximum acceleration parameter, it was always set equal to 2.00. No satisfactory theoretical method was found to estimate the minimum acceleration parameter, and the selection of it is discussed under "Comparison of Solution Methods". The number and values of the other parameters were found from a scheme given by Varga (1962, p. 226-229) for generating approximate values for the linear, commutative case:

$$\left.\begin{aligned} m &= 1.309 \log \left(\frac{\omega_{max}}{\omega_{min}} \right) \\ \omega_p &= \omega_{min} (2.41)^{2p-1}, \qquad 1 \le p \le m \end{aligned}\right\} \tag{34}$$

The term m is rounded to the nearest integer and is two less than the total number of parameters used, ω_{max} and ω_{min} constituting the remaining two. When used in equations 32 and 33, the parameter was changed at each iteration, i.e., at k, k+1, k+2, etc.

Line successive over-relaxation (SLOR) is an iterative solution procedure for which the equations for internal node points of lines oriented in the z (or j) direction can be written

$$(K_rA_x)^{(k,n+1/2)}_{i+1/2,j} (h^{(k,n+1)}_{i+1,j} - \hat{h}^{(k+1,n+1)}_{i,j}) - (K_rA_x)^{(k+1,n+1/2)}_{i-1/2,j} (\hat{h}^{(k+1,n+1)}_{i,j} - h^{(k+1,n+1)}_{i-1,j})$$

$$+(K_rA_z)^{(k,n+1/2)}_{i,j+1/2} (\hat{h}^{(k+1,n+1)}_{i,j+1} - \hat{h}^{(k+1,n+1)}_{i,j}) - (K_rA_z)^{(k,n+1/2)}_{i,j-1/2} (\hat{h}^{(k+1,n+1)}_{i,j} - \hat{h}^{(k+1,n+1)}_{i,j-1})$$

$$= \frac{(V_b)_{i,j}}{\Delta t^D} \left[(S_w)^{(k,n+1/2)}_{i,j} (S_r)_{ir} - \left(\frac{\Delta S_a^D}{\Delta p_h} \right)^{(k,n+1/2)}_{i,j} \right] (\hat{h}^{(k+1,n+1)}_{i,j} - h^{(n)}_{i,j}) \tag{35}$$

and

$$h^{(k+1,n+1)}_{i,j} = \omega\, (\hat{h}^{(k+1,n+1)}_{i,j} - h^{(k,n+1)}_{i,j}) + h^{(k,n+1)}_{i,j}, \qquad 1 \le \omega < 2 \tag{36}$$

The equation for points lying on a region boundary is identical except the terms for flow in the r direction and the storage change term (the right side of the equation) are composed of two terms, one for each region. For example, for region boundary point (i,j)

$$(K_r A_x)^{(n+1/2)}_{i+1/2,j} \quad (h_{i+1,j} - h_{i,j})^{(n+1)}$$

$$= \left[(K_r A_x)_{ir} + (K_r A_x)_{ir+1} \right]^{(n+1/2)}_{i+1/2,j} \; (h_{i+1,j} - h_{i,j})^{(n+1)}$$

As can be seen from equations 35 and 36, the procedure is to solve simultaneously for all h's along a line using the most recent h's calculated on adjacent lines as knowns. After all h's on a line are calculated, they are over-relaxed or extrapolated using ω. The coefficients of the h's for the line are updated using the extrapolated h's so that they are also the most recent possible. Convergence at time step (n+1) has resulted when

$$|h^{(k+1)}_{i,j} - h^{(k)}_{i,j}|^{(n+1)} \quad \leq \quad \varepsilon$$

As for ADIPIT, selection of ω materially affects convergence rate, and Varga (1962, pp. 283-297) outlines methods of estimating it for linear difference equations. For the nonlinear problems, however, the optimum ω is usually selected by trial and error (McCracken and Dorn, 1964, p. 377).* It was always between 1.3 and 1.6 for the problems investigated in this study.

For ADIPIT and SLOR, S^D_a and K_r were changed at each iteration. However, in a manner similar to ADIP, divergence sometimes occurred if the values as computed directly from h were used for the next iteration. Therefore, equation 31 was used to interpolate S^D_a, and K_r was obtained from the interpolated S^D_a.

---

* See addendum

It was found desirable to modify the basic equations for the three solution methods. Instead of writing $h^{(k+1)}$ as an unknown in each equation, it was replaced by

$$h^{(k+1)} = h^{(k)} + \Delta h^{(k+1)} \tag{37}$$

where $\Delta h^{(k+1)}$ is the displacement, or the change in h accomplished by one iteration. With equation 37 replacing $h^{(k+1)}$ in the finite difference equations, $\Delta h^{(k+1)}$ is the unknown, and terms involving $h^{(k)}$ can be treated as knowns. This procedure, described fully in McCracken and Dorn (1964, pp. 243-246), accomplishes two main things. First, a higher degree of accuracy is attainable using fewer decimal places than could be gained using the original equations because $\Delta h^{(k+1)}$ can be relaxed to very near zero. Second, it was found necessary to test the residual for each equation as well as the displacement when checking convergence, and the residual is obtained directly as the sum of all known terms if equation 37 is used. The residual had to be checked independently of the displacement because of the change in mesh volumes radially from the well. The same error in h can produce a much larger error in residual for a large mesh volume far from the well than for a small one near the well.

For each iteration all three methods yield tridiagonal matrix equations written in terms of the unknown displacements. The equations can be solved by a very efficient triangular decomposition technique, the Thomas method (Bruce, Peaceman, Rachford, and Rice, 1953, p. 79, Peaceman and Rachford, 1955, p. 34, McCarty and Barfield, 1958, p. 142, Lapidus, 1962, pp. 254-255).

The method and its application to equations of the type used here are detailed in the above references and will not be explored further here.

The boundary condition below the water level in the well bore was that of a known, constant head. However, this known head has to be interpreted as the head necessary to yield a constant specified discharge. Because the governing partial differential equation is nonlinear, superposition of solutions to correct the head to produce the desired discharge as was employed by Neuman and Witherspoon (1969, pp. 104-108) to analyze flow to a well in confined strata could not be used. An iterative solution method was employed in this study. At the beginning of the first two time steps an initial approximation for head $h_w^{(k)}$, k=1, was obtained from Darcy's law for purely radial flow

$$h_w^{(1)} = h_{2,jb}^{(old)} - Q^D \left\{ \frac{r_2 - r_1}{2\pi r_1 \left[\sum_{(ir)} (Kb)_{ir}\right]} \right\} \tag{38}$$

where jb refers to the j coordinate of the bottom of the well, and $h^{(old)}$ refers to the value of h at the end of the last time level. The uppermost b_{ir} used was calculated as the difference between the water level in the well bore and the z coordinate at the region boundary just below the water level. Also, k as used for the present iteration procedure should not be confused with k used previously as iteration number in the solution of the difference equations. Assuming h_w as calculated by equation 38, the solution to the unknown head distribution was made, then the actual discharge yielded by h_w was calculated from

$$(Q_c^D)^{(k)} = \sum_{j=jb}^{js} (Q_{1,j-1/2} - Q_{1,j+1/2} - Q_{3/2,j} - \frac{\Delta ST}{\Delta t^D}) \tag{39}$$

where

$$\Delta ST = (V_b)_{i,j} \left[(S_w)_{i,j}^{(n+1/2)} (S_r)_{ir} (h_{i,j}^{(n+1)} - (h_{i,j}^{(n)}) + (S_a^D)_{i,j}^{(n)} - (S_a^D)_{i,j}^{(n+1)} \right].$$

The time step superscripts to be used with the Q's depend on the solution method being used. If

$$|(Q_c^D)^{(k)} - Q^D| \quad > \quad \varepsilon_Q$$

then a new trial head $h_w^{(k+1)}$, was obtained from

$$h_w^{(k+1)} = \frac{(h_w^{(k)} - h_w^{(k-1)})}{\left[(Q_c^D)^{(k)} - (Q_c^D)^{(k-1)}\right]} \left[Q^D - (Q_c^D)^{(k-1)} \right] + h_w^{(k-1)} \tag{40}$$

The solution to the unknown head distribution was made again, and Q_c^D was calculated and tested for convergence. If convergence was not obtained, equation 40 was reapplied, etc. The terms $(Q_c^D)^{(k-1)}$ and $h_w^{(k-1)}$ for the first iteration, k=1, were obtained from the last time level:

$$\left.\begin{aligned} h_w^{(k-1)} &= h_w^{(old)} \\ \text{and} \quad (Q_c^D)^{(k-1)} &= \left(\frac{1 - h_w^{(old)}}{1 - h_w^{(k)}} \right) Q^D \end{aligned}\right\} \tag{41}$$

The above iterative procedure for ADIP was employed only at time levels where flow components in the r direction were implicit. Discharges calculated for all mesh volumes were used explicitly as known quantities for solution in the z direction. Convergence for all solution methods was obtained in one, two, or at most three iterations.

After the second time step, all hydraulic heads were extrapolated, and new values of S_a^D and K_r were calculated from them. This extrapolation of heads, which provided a better set of heads and coefficients to start the iterations than resulted from using the unextrapolated values, conformed to the basic logarithmic nature of problems involving flow to a well:

$$h_{i,j}^{(n+1)} = \frac{\log(t^{(n+1)}/t^{(n-1)})}{\log(t^{(n)}/t^{(n-1)})} \quad (h_{i,j}^{(n)} - h_{i,j}^{(n-1)}) + h_{i,j}^{(n-1)} \tag{42}$$

Here $h_{i,j}^{(n+1)}$ is the extrapolated value for time step (n+1) (or (n+1/2) for ADIP). The extrapolated term $h_{1,jb}^{(n+1)}$ was used as the initial estimate for the known head boundary condition in the well bore. For all except early values of time, this procedure often resulted in only one iteration to obtain the value of h_w to yield Q^D.

The location of the seepage surface was another initially unknown quantity for each time step, and it's determination was incorporated into the iteration sequence for solving the difference equations. At the beginning of the sequence, the top of the seepage surface was set at one node point below the uppermost node point with zero or positive pressure. Five iterations were completed with this boundary condition, the node points were checked, the top of the seepage surface was reset at the uppermost node point with zero or positive pressure, and the iteration sequence was completed. This procedure appeared to yield the correct elevation of the seepage surface for all time levels.

At the end of each full time step (i.e., at integer values of n), a total material balance check was made to ascertain whether total mass was being conserved in the system. The basic balance equation is

$$\frac{-\sum\limits_{(i,j)} (\Delta ST)}{\Delta t^D (Q_c^D - Q_e^D)} \approx 1 \tag{43}$$

The mass balance ratio was always within .002 of 1.00 and was usually much closer when using ADIPIT or SLOR.

COMPARISON OF SOLUTION METHODS

Because ADIP and ADIPIT have only been applied to problems involving wells that fully penetrate single elastic unconfined aquifers, comparisons were limited to this type of flow system. See table 1 for a list of the test problems.

The ADIP was found to be unsatisfactory for most problems investigated at least in part because the serial nature of the solution for flow components in the r and z directions caused a violation of the mechanics of flow at small values of time. The initial condition was a uniform head distribution; therefore, solution at n=1/2 for flow in the r direction used the initial condition explicitly for flow in the z direction. Because no flow can take place under uniform head conditions, no drainage or desaturation could take place between n=0 and n=1/2, no matter what size time step was used. Flow was purely radial, and, due to all discharge at the well bore being derived from elastic storage, the drawdown water table spread too far. (If the solution would have been made for flow in the z direction using the initial condition for flow in the r direction, no flow could exist across the well bore!)

Solution at $n=1$ for flow in the z direction produced too much water from desaturation above the water table because vertical flow could take place as far from the well as the drawdown water table had spread during the first half time increment. At $n=3/2$ the head in the well bore increased, apparently to compensate for the excess of water yielded from storage over what was withdrawn as well discharge during the last time step. These oscillations usually continued through the solution, and sometimes the solution became unstable. In an effort to combat the oscillation problem, the initial time step was made very small (.0005 minutes). In order to maintain stability, the time step could not be increased abruptly, however, and many time steps were needed to obtain a solution over a pumping period of several hours or longer. Briggs and Dixon (1968) found that the time step size for ADIP had to be severely restricted to dampen oscillations of the solution even for a simple linear case involving a well pumping in a rectangular aquifer with constant thickness and constant pressure boundaries. They concluded that, because of the time step restriction, ADIP was often not a satisfactory solution method.

The ADIPIT and SLOR methods were stable and yielded nearly the same solutions for all problems investigated (figures 3 and 4). In addition, they converged with a similar number of iterations (see table 2), although ADIPIT sometimes used slightly fewer. However, each iteration for ADIPIT involves two mesh sweeps, one in each direction; whereas, SLOR requires only one with the result that SLOR used less computer time.

Another problem with ADIPIT involved the selection and use of the acceleration parameters. Convergence rate was found to be sensitive to the number of parameters used and the value of the minimum parameter. The number was selected by equation 34, and it was found that if more parameters were used the convergence rate was slower. The minimum parameter had to be selected by trial and error. Values between .001 and .03 usually produced satisfactory convergence, but proper selection within the range had to be made for each problem. Also, as the time step size was increased during the course of a problem, the value of ω_{min} often had to be decreased or the number of iterations necessary for convergence became large, sometimes 50 or greater. In contrast, selection of ω for SLOR was easier because only one value was needed at each time step, and often it could be varied over a range of about ± 0.05 without altering the number of iterations greatly (figure 5). In conclusion, although both ADIPIT and SLOR produced satisfactory solutions for the problems investigated, SLOR was faster and easier to use.

ACKNOWLEDGMENTS

This study, which was initiated as post-doctorate work at the Pennsylvania State University, was completed at The Hydrologic Engineering Center, US Army Corps of Engineers. Support for the initial portion of the study was granted by the Pennsylvania State University through the Institute for Research on Land and Water Resources and by the Office of Water Resources Research, United States Department of Interior. The major portion of the study was financed by The Hydrologic Engineering Center where the author is employed. The author would also like to thank Dr. D.A.T. Donohue, who coauthored the initial report on the study, for his guidance and Drs. P.W. Hughes and J.F. Harsh, and Mr. John Peters for reviewing the manuscript for the present report.

The opinions expressed herein are those of the author and do not necessarily reflect the policy of the Corps of Engineers.

REFERENCES CITED

Aris, Rutherford, 1962, Vectors, tensors, and the basic equations of fluid mechanics: Englewood Cliffs, New Jersey, Prentice-Hall, 286 pp.

Breitenbach, E.A., Thurnau, D.H., and van Poolen, H.K., 1968a, Immiscible fluid flow simulator: Soc. Petroleum Engineers Symposium on Numerical Simulation of Reservoir Performance, Dallas, Apr. 22-23, 1968, preprint SPE 2019, 24 pp.

__________ 1968b, The fluid flow simulation equations: Soc. Petroleum Engineers Symposium on Numerical Simulation of Reservoir Performance, Dallas, Apr. 22-23, 1968, preprint SPE 2020, 11 pp.

__________ 1968c, Solution of the immiscible fluid flow simulation equations: Soc. Petroleum Engineers Symposium on Numerical Simulation of Reservoir Performance, Dallas, Apr. 22-23, 1968, preprint SPE 2021, 13 pp.

Briggs, J.E., and Dixon, T.N., 1968, Some practical considerations in the numerical solution of two-dimensional reservoir problems: Soc. Petroleum Engineers Jour., v. 8, no. 2, pp. 185-194.

Bruce, G.H., Peaceman, D.W., Rachford, H.H., and Rice, J.D., 1953, Calculation of unsteady gas flow through porous media: AIME Trans., v. 198, pp.79-92.

Childs, E.C., 1960, The non-steady state of the water table in drained land: Jour. Geophys. Research, v. 65, no. 2, pp. 780-782.

Coats, K.H., Nielsen, R.L., Terhune, M.H., and Weber, A.G., 1967, Simulation of three-dimensional, two-phase flow in oil and gas reservoirs: Soc. Petroleum Engineers Jour., v. 7, no. 4, pp. 377-388.

Cooley, R.L., and Donohue, D.A.T., 1969, Numerical simulation of unconfined flow into a single pumping water-well using two-phase flow theory: Pennsylvania State University, Inst. for Research on Land and Water Resources Tech. Completion Rept., 25 pp.

Cooper, H.H., Jr., 1966, The equation of ground water flow in fixed and deforming coordinates: Jour. Geophys. Research, v. 71, no. 20, pp. 4785-4790.

Corey, A.T., 1954, The interrelation between gas and oil relative permeabilities: Producers Monthly, v. 19, no. 1, pp. 38-41.

Douglas, Jim, Jr., 1962, Alternating direction methods for three space variables: Numerische Mathematik, v. 4. pp. 41-63.

Douglas, Jim, Jr., Peaceman, D.W., and Rachford, H.H., Jr., 1959, A method for calculating multi-dimensional immiscible displacement: Soc. Petroleum Engineers of AIME Trans., v. 216, pp. 297-308.

Fagin, R.G., and Stewart, C.H., Jr., 1966, A new approach to the two-dimensional multiphase reservoir simulator: Soc. Petroleum Engineers Jour., June, 1966, pp. 175-182.

Freeze, R.A., 1969, The mechanism of natural ground water recharge and discharge. 1. One-dimensional, vertical, unsteady, unsaturated flow above a recharging or discharging ground water flow system: Water Resources Research, v.5, no. 1, pp. 153-171.

Klute, A., 1969, The movement of water in soils: International Seminar for Hydrology Professors, Univ. of Illinois, Urbana, July 13-15, 1969, 69 pp.

Lamb, H., 1945, Hydrodynamics: New York, Dover, 738 pp.

Lapidus, Leon, 1962, Digital computation for chemical engineers: New York, McGraw-Hill, 407 pp.

McCracken, D.D., and Dorn, W.S., 1964, Numerical methods and fortran programming: New York, John Wiley and Sons, 457 pp.

McCarty, D.G., and Barfield, E.C., 1958, The use of high speed computers for predicting flood-out patterns: Soc. Petroleum Engineers of AIME Trans., v. 213, pp. 139-145.

Neuman, S.P., and Witherspoon, P.A., 1969, Transient flow of ground water to wells in multiple-aquifer systems: Univ. of California, Berkeley, Department of Civil Engineering Pub. 69-1, 181 pp.

Peaceman, D.W., and Rachford, H.H., Jr., 1955, The numerical solution of parabolic and ellipic differential equations: Soc. Indus. Appl. Math. Jour., v. 3, no. 1, pp. 28-41.

Pearcy, Carl, 1962, On convergence of alternating direction procedures: Numerische Mathematik, v. 4, pp. 172-176.

Rubin, J., 1968, Theoretical analysis of two-dimensional, transient flow of water in unsaturated and partly unsaturated soils: Soil Science Soc. America Proc., v. 32, no. 5, pp. 607-615.

Smith, G.D., 1965, Numerical solution of partial differential equations: New York, Oxford, 179 pp.

Spanier, J., 1967, Alternating direction methods applied to heat conduction problems, chap. 11 in Ralston, Anthony, and Wilf, H.S., Mathematical methods for digital computers, v. 2: New York, John Wiley and Sons, 287 pp.

Stallman, R.W., 1961, Relation between storage changes at the water table and observed water level changes: U.S. Geol. Survey Prof. Paper 424-B, pp. B39-B40.

Taylor, G.S., and Luthin, J.N., 1969, Computer methods for transient analysis of water-table aquifers: Water Resources Research, v. 5, no. 1, pp. 144-152.

Varga, R.S., 1962, Matrix iterative analysis: Englewood Cliffs, New Jersey, Prentice-Hall, 322 pp.

Welge, H.J., and Weber, A.G., 1964, Use of two-dimensional methods for calculating well coning behavior: Soc. Petroleum Engineers Jour., v. 231, pp. 345-355.

APPENDIX

I. NOTATION

A - constant for relationship of S_a^D to p_h; general flow coefficient

A_x - coefficient for flow in the r direction

A_z - coefficient for flow in the z direction

B - thickness of a rock property region

b - dimensionless thickness of a rock property region $= \frac{B}{H_o}$

b_T - dimensionless thickness of total flow system $= \frac{B_T}{H_o}$

c - water compressibility; exponent for relationship of S_a^D to p_h

c_n - pore compressibility

d - exponent for relationship of K_r to S_a

g - gravitational constant

H - hydraulic head $= P_h + Z$

H_o - initial hydraulic head

h - dimensionless hydraulic head $= \frac{H}{H_o}$

h_e - dimensionless head at external lateral boundary = 1

h_w - dimensionless head below water level in well bore

J - $\frac{\partial z}{\partial \zeta}$, Jacobian

K - hydraulic conductivity

K_o - hydraulic conductivity of reference rock property region

K^D - dimensionless conductivity $= \frac{K}{K_o}$

K_c - capillary conductivity

K_r - relative conductivity $= \frac{K_c}{K}$

N - direction normal to S

n - porosity

P - water pressure

P_a - air pressure

P_c - capillary pressure = $P_a - P$

P_h - water pressure head = $\frac{P}{\rho g}$

p_h - dimensionless pressure head = $\frac{P_h}{H_o}$

Q - discharge at well bore; dimensionless discharge at any point

Q^D - dimensionless discharge at well bore = $\frac{Q}{K_o H_o^2}$

Q_c^D - calculated dimensionless discharge at well bore using h_w

Q_e^D - dimensionless discharge across external lateral boundary

R - radius from well center

r - dimensionless radius = $\frac{R}{H_o}$

r_e - dimensionless radius of external lateral boundary

r_w - dimensionless radius of well bore

S - surface area

S_ℓ - surface of mesh volume element

S_r - storage ratio = $\frac{S_s H_o}{S_y}$

S_s - specific storage

S_y - specific yield = $n\ S_{ar}$

$(S_y)_o$ -specific yield of reference rock property region

S_y^D - specific yield ratio = $\frac{S_y}{(S_y)_o}$

S_a - air saturation = $1 - S_w$

S_a^D - normalized air saturation = $\frac{S_a}{S_{ar}}$

S_{ar} - residual air saturation

S_w - water saturation

t - time

t^D - dimensionless time = $\frac{K_o t}{(S_y)_o H_o}$

$\vec{v}$ - discharge of water per unit area

V - volume

V_b - volume coefficient for storage change

V_ℓ - mesh volume element

V_o - fixed initial volume element, $\Delta x \Delta y \Delta \zeta$

$V(t)$ - volume element that deforms with time

V_v - volume of voids

w_g - velocity of grains in the Z direction

Z - deforming elevation above the bottom of the flow system

z - dimensionless deforming elevation = $\frac{Z}{H_o}$

z_B - dimensionless elevation of well bottom

z_s - dimensionless elevation of top of seepage surface at well bore

ε - convergence criterion (10^{-7})

ε_Q - convergence criterion for discharge calculations iterations = $.001Q^D$

ζ - fixed initial vertical coordinate

ρ - mass density of water

ω - acceleration parameter

ω_s - interpolation parameter for S_a^D interpolation

Indices

i - node point number in r direction

ir - rock property region number

j - node point number in z direction

jb - j number of well bottom

js - j number of top of seepage surface

k - iteration number

n - time step number

II. DERIVATION OF SPECIFIC STORAGE

From the concept of volume element V(t) deforming elastically in response to pressure changes,

$$dV(t) = JdV_o \tag{1}$$

(Cooper, 1966, p. 4788, Aris, 1962, p. 83). Using equation 1 and the relationship

$$\frac{1}{J}\frac{\partial J}{\partial t} = \frac{\partial w_g}{\partial z} \tag{2}$$

(Cooper, 1966, p. 4788), the integral involving the rate of change of storage with time over V(t) may be transformed to an integral over V_o:

$$\frac{\partial}{\partial t} \iiint\limits_{V(t)} S_w \rho n dV$$

$$= \frac{\partial}{\partial t} \iiint\limits_{V_o} S_w \rho n J dV$$

$$= \iiint\limits_{V_o} \left[\rho n J \frac{\partial S_w}{\partial t} + S_w J \left(n \frac{\partial \rho}{\partial t} + \rho \frac{\partial n}{\partial t} + \rho n \frac{1}{J} \frac{\partial J}{\partial t} \right) \right] dV$$

$$= \iiint\limits_{v(t)} \left[\rho n \frac{\partial S_w}{\partial t} + S_w \left(n \frac{\partial \rho}{\partial t} + \rho \frac{\partial n}{\partial t} + \rho n \frac{\partial w_g}{\partial z} \right) \right] dV$$

The compressibility of water is defined as

$$c = -\frac{1}{V}\frac{dV}{dP}$$

$$= \frac{1}{\rho}\frac{d\rho}{dP} . \tag{4}$$

Taking the time derivative

$$c\rho \frac{\partial P}{\partial t} = \frac{\partial \rho}{\partial t} . \tag{5}$$

Aquifer compressibility can be defined

$$c_n = \frac{1}{\delta V_v}\frac{d(\delta V_v)}{dP} . \tag{6}$$

Therefore,

$$c_n = \frac{1}{n\delta V(t)}\frac{d(n\delta V(t))}{dP}$$

$$= \frac{1}{n\delta V(t)}\left[\delta V(t)\frac{dn}{dP} + n\frac{d(\delta V(t))}{dP}\right]$$

$$= \frac{1}{n}\frac{dn}{dP} + \frac{1}{\delta V(t)}\frac{d(\delta V(t))}{dP}$$

$$= \frac{1}{n}\frac{dn}{dP} + \frac{1}{J\delta V_o}\frac{d(J\delta V_o)}{dP}$$

$$= \frac{1}{n}\frac{dn}{dP} + \frac{1}{J}\frac{dJ}{dP} . \tag{7}$$

Multiplying by ρn and taking the time derivative, there results

$$\rho n c_n \frac{\partial P}{\partial t} = \rho\frac{\partial n}{\partial t} + \rho n\frac{\partial w_g}{\partial z} . \tag{8}$$

Using equations 5 and 8, equation 3 thus becomes

$$\iiint\limits_{V(t)} \left[\rho n \frac{\partial S_w}{\partial t} + S_w \rho n (c+c_n)\frac{\partial P}{\partial t}\right] \quad dV$$

$$= \iiint\limits_{V(t)} \left[\rho n \frac{\partial S_w}{\partial t} + S_w \rho^2 g n \; (c + c_n) \frac{\partial H}{\partial t} \right] dV$$

$$= \iiint\limits_{V(t)} \left[\rho n \frac{\partial S_w}{\partial t} + S_w \rho S_s \frac{\partial H}{\partial t} \right] dV \qquad (9)$$

ADDENDUM

Further investigation has yielded a method of generating ω internally for each time step except the first. At the end of a time step, the following quantities are computed:

$$G_\omega = \left[\sum_{k=8}^{it} \left| \frac{\max(\Delta h_k)}{\max(\Delta h_{k-1})} \right| \right] \Big/ it \tag{1}$$

$$G'_\omega = \left[\sum_{k=8}^{it} \frac{\max(\Delta h_k)}{\max(\Delta h_{k-1})} \right] \Big/ it \tag{2}$$

$$G = \frac{[G_\omega + \omega_{old} - 1]^2}{G_\omega \, \omega_{old}^2} \tag{3}$$

Here ω_{old} is the acceleration parameter used for the time step just completed, and (it) is the number of iterations for the last cycle of iterations. Using G computed from equation 3, a new trial acceleration parameter, ω', is computed:

$$\omega' = \frac{2}{1+\sqrt{1-G}} \tag{4}$$

If

$$|G_\omega - G'_\omega| > 0.1 \tag{5}$$

then ω_{old} is adjusted:

$$\omega = \omega_{old} - (\omega' - \omega_{old}) \tag{6}$$

Equation 3 and 4 represent theoretical relationships between the spectral radius of the block Gauss-Seidel matrix, G, and the spectral radius of the block successive overrelaxation matrix, G_ω, with ω_{old} as the acceleration parameter (Varga, 1962, pp. 105-111). The method outlined by equations 1 through 4 computed close to the optimum ω if convergence of the maximum displacement was monotonic (i.e., if $G_\omega = G'_\omega$). However, if the solution oscillated during iterations, then the ω_{old} used was too large, and it was reduced for the next time step using equation 6.

Table 1. Test problems for comparison of the ADIPIT and SLOR

Problem number	Q (gpm)	K (gpd/ft^2)	S_y	S_s (ft^{-1})	A	S_{ar}	c	d	H_o (ft)	r_e (ft)	r_w (ft)
1	5	1000	.225	.00001	2	.75	3	1	18	256	.5
2	5	1000	.225	.00001	2	.75	3	1	18	1280	.5
3	50	1000	.225	.00001	2	.75	3	1	18	256	.5
4	50	1000	.225	.00001	2	.75	3	1	18	1280	.5
5	1000	2720	.032	.00002	2	.15	3	1	100	4000	.67
6	1000	2720	.032	.00002	500,000	.15	5	4	100	4000	.67

Table 2. Total number of iterations at each time step for 6 time steps, test problem no. 4.

Time step number	h_w	no. of iterations ADIPIT	SLOR
1	.9646*	17	25
	.8891	35	26
	.8916	22	19
2	.8732	26	26
	.8813	26	24
	.8882	26	24
3	.8858	26	25
	.8864	26	25
	.8867	26	25
4	.8855	26	25
5	.8843	26	25
	.8841	26	25
6	.8828	27	26
	.8826	25	26

* These values differed in the fifth or sixth decimal place between methods.

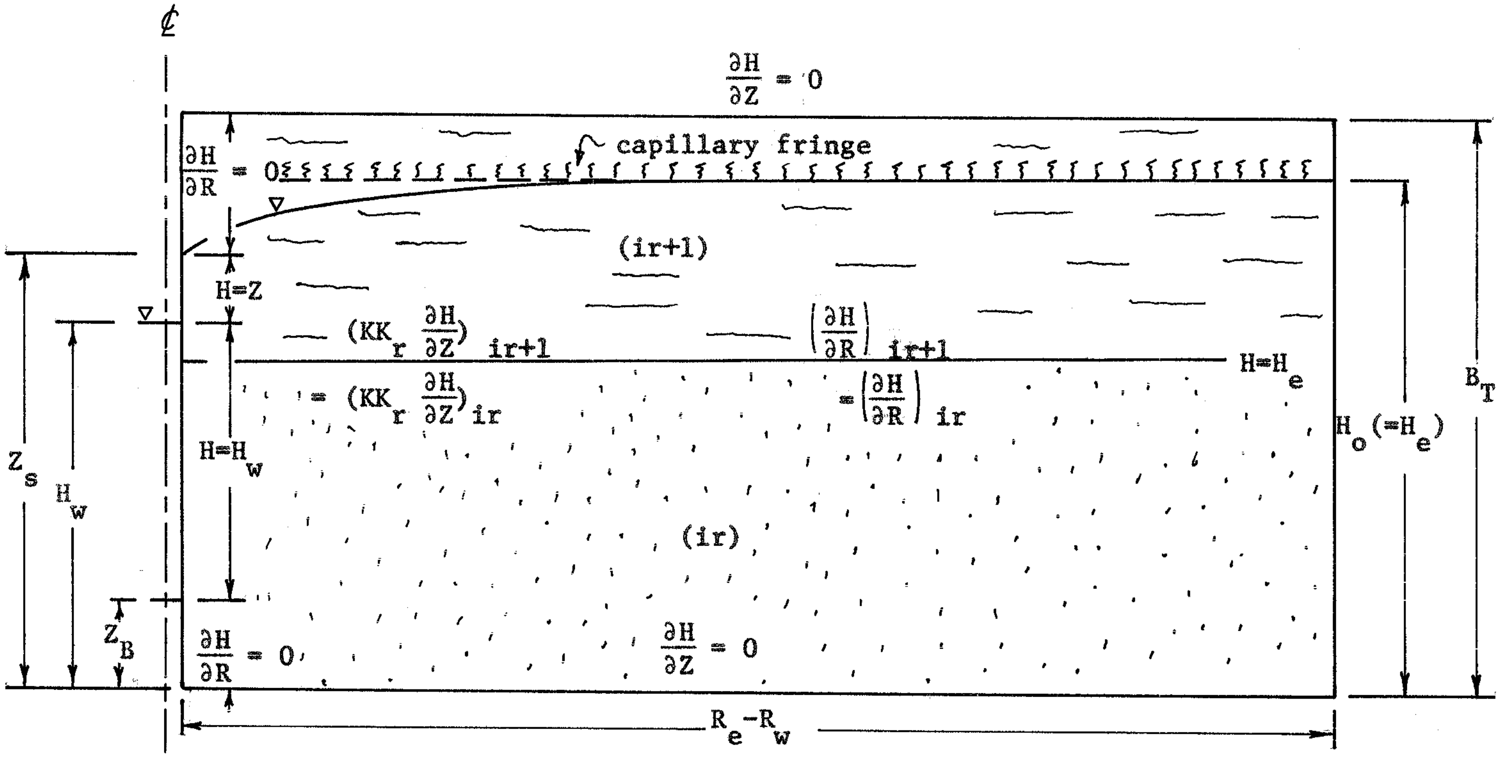

Figure 1. Geometry and boundary conditions for flow to a well completely penetrating an upper rock unit (ir+1) and partially penetrating the lower (ir).

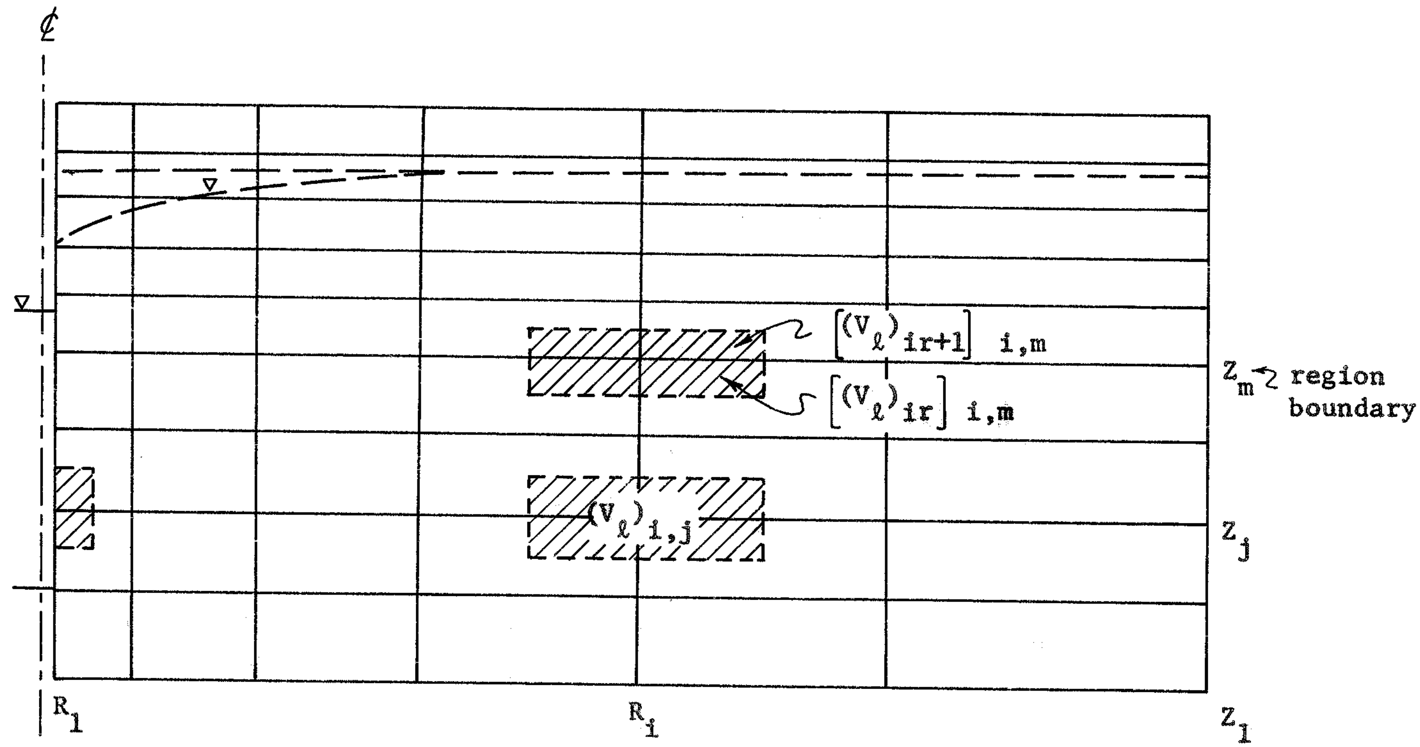

Figure 2. Schematic finite difference mesh and selected mesh volumes for the case depicted in figure 1.

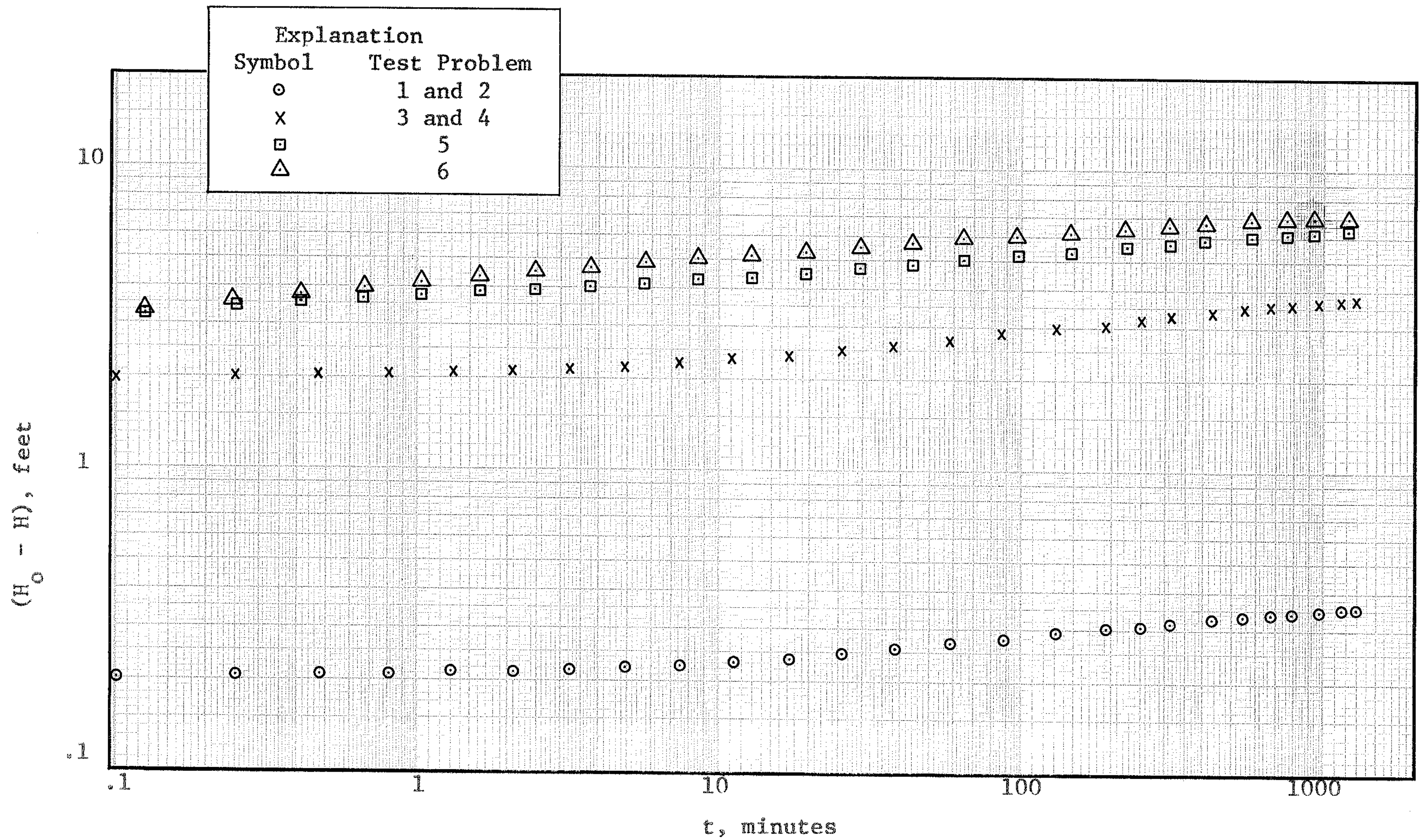

Figure 3. Graphs of time vs drawdown at the well bore for the test problems solved by ADIPIT and SLOR (see table 1 for information about the problems). Differences in values of drawdown calculated by the two methods could not be shown at the scale of the graph.

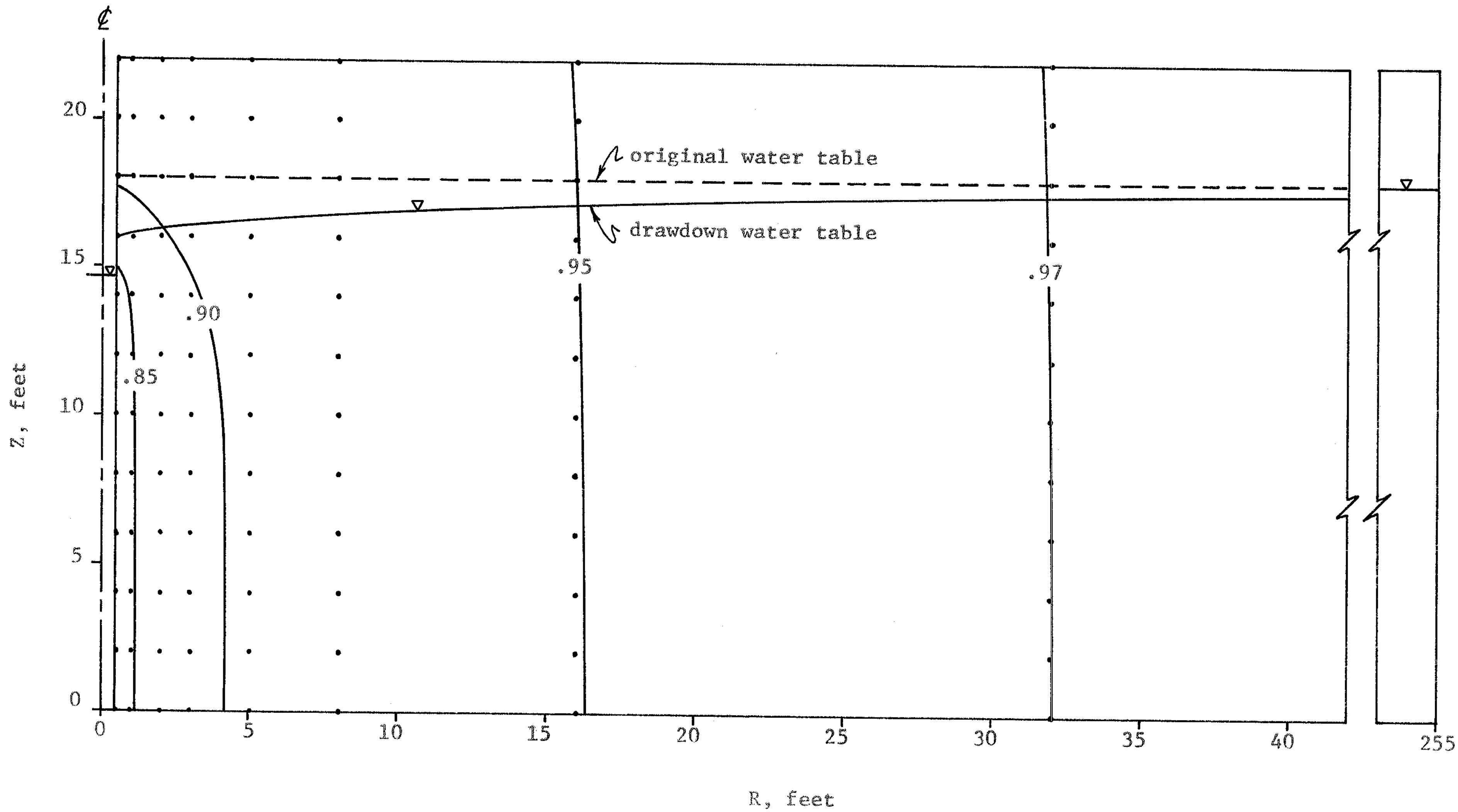

Figure 4. Flow system and mesh point configuration at t = 311 minutes for test problems no. 3. Contours represent the fraction of the original hydraulic head (18 feet) remaining at time t.

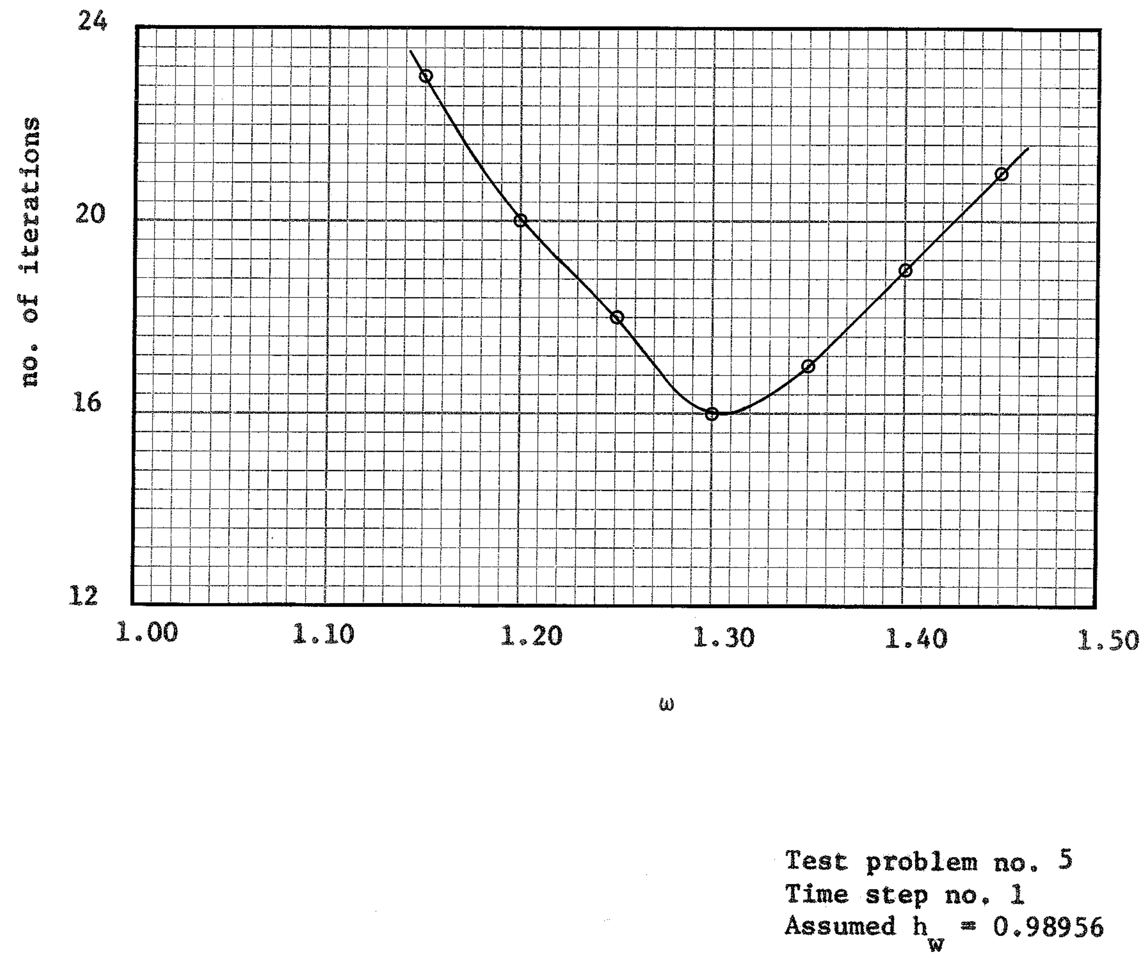

Figure 5. Number of iterations for each assumed ω needed to reduce the maximum displacement, $|h^{(k+1)} - h^{(k)}|_{max}$, to 10^{-7} using SLOR.

Technical Paper Series

TP-1 Use of Interrelated Records to Simulate Streamflow
TP-2 Optimization Techniques for Hydrologic Engineering
TP-3 Methods of Determination of Safe Yield and Compensation Water from Storage Reservoirs
TP-4 Functional Evaluation of a Water Resources System
TP-5 Streamflow Synthesis for Ungaged Rivers
TP-6 Simulation of Daily Streamflow
TP-7 Pilot Study for Storage Requirements for Low Flow Augmentation
TP-8 Worth of Streamflow Data for Project Design - A Pilot Study
TP-9 Economic Evaluation of Reservoir System Accomplishments
TP-10 Hydrologic Simulation in Water-Yield Analysis
TP-11 Survey of Programs for Water Surface Profiles
TP-12 Hypothetical Flood Computation for a Stream System
TP-13 Maximum Utilization of Scarce Data in Hydrologic Design
TP-14 Techniques for Evaluating Long-Tem Reservoir Yields
TP-15 Hydrostatistics - Principles of Application
TP-16 A Hydrologic Water Resource System Modeling Techniques
TP-17 Hydrologic Engineering Techniques for Regional Water Resources Planning
TP-18 Estimating Monthly Streamflows Within a Region
TP-19 Suspended Sediment Discharge in Streams
TP-20 Computer Determination of Flow Through Bridges
TP-21 An Approach to Reservoir Temperature Analysis
TP-22 A Finite Difference Methods of Analyzing Liquid Flow in Variably Saturated Porous Media
TP-23 Uses of Simulation in River Basin Planning
TP-24 Hydroelectric Power Analysis in Reservoir Systems
TP-25 Status of Water Resource System Analysis
TP-26 System Relationships for Panama Canal Water Supply
TP-27 System Analysis of the Panama Canal Water Supply
TP-28 Digital Simulation of an Existing Water Resources System
TP-29 Computer Application in Continuing Education
TP-30 Drought Severity and Water Supply Dependability
TP-31 Development of System Operation Rules for an Existing System by Simulation
TP-32 Alternative Approaches to Water Resources System Simulation
TP-33 System Simulation of Integrated Use of Hydroelectric and Thermal Power Generation
TP-34 Optimizing flood Control Allocation for a Multipurpose Reservoir
TP-35 Computer Models for Rainfall-Runoff and River Hydraulic Analysis
TP-36 Evaluation of Drought Effects at Lake Atitlan
TP-37 Downstream Effects of the Levee Overtopping at Wilkes-Barre, PA, During Tropical Storm Agnes
TP-38 Water Quality Evaluation of Aquatic Systems
TP-39 A Method for Analyzing Effects of Dam Failures in Design Studies
TP-40 Storm Drainage and Urban Region Flood Control Planning
TP-41 HEC-5C, A Simulation Model for System Formulation and Evaluation
TP-42 Optimal Sizing of Urban Flood Control Systems
TP-43 Hydrologic and Economic Simulation of Flood Control Aspects of Water Resources Systems
TP-44 Sizing Flood Control Reservoir Systems by System Analysis
TP-45 Techniques for Real-Time Operation of Flood Control Reservoirs in the Merrimack River Basin
TP-46 Spatial Data Analysis of Nonstructural Measures
TP-47 Comprehensive Flood Plain Studies Using Spatial Data Management Techniques
TP-48 Direct Runoff Hydrograph Parameters Versus Urbanization
TP-49 Experience of HEC in Disseminating Information on Hydrological Models
TP-50 Effects of Dam Removal: An Approach to Sedimentation
TP-51 Design of Flood Control Improvements by Systems Analysis: A Case Study
TP-52 Potential Use of Digital Computer Ground Water Models
TP-53 Development of Generalized Free Surface Flow Models Using Finite Element Techniques
TP-54 Adjustment of Peak Discharge Rates for Urbanization
TP-55 The Development and Servicing of Spatial Data Management Techniques in the Corps of Engineers
TP-56 Experiences of the Hydrologic Engineering Center in Maintaining Widely Used Hydrologic and Water Resource Computer Models
TP-57 Flood Damage Assessments Using Spatial Data Management Techniques
TP-58 A Model for Evaluating Runoff-Quality in Metropolitan Master Planning
TP-59 Testing of Several Runoff Models on an Urban Watershed
TP-60 Operational Simulation of a Reservoir System with Pumped Storage
TP-61 Technical Factors in Small Hydropower Planning
TP-62 Flood Hydrograph and Peak Flow Frequency Analysis
TP-63 HEC Contribution to Reservoir System Operation
TP-64 Determining Peak-Discharge Frequencies in an Urbanizing Watershed: A Case Study
TP-65 Feasibility Analysis in Small Hydropower Planning
TP-66 Reservoir Storage Determination by Computer Simulation of Flood Control and Conservation Systems
TP-67 Hydrologic Land Use Classification Using LANDSAT
TP-68 Interactive Nonstructural Flood-Control Planning
TP-69 Critical Water Surface by Minimum Specific Energy Using the Parabolic Method

TP-70 Corps of Engineers Experience with Automatic Calibration of a Precipitation-Runoff Model
TP-71 Determination of Land Use from Satellite Imagery for Input to Hydrologic Models
TP-72 Application of the Finite Element Method to Vertically Stratified Hydrodynamic Flow and Water Quality
TP-73 Flood Mitigation Planning Using HEC-SAM
TP-74 Hydrographs by Single Linear Reservoir Model
TP-75 HEC Activities in Reservoir Analysis
TP-76 Institutional Support of Water Resource Models
TP-77 Investigation of Soil Conservation Service Urban Hydrology Techniques
TP-78 Potential for Increasing the Output of Existing Hydroelectric Plants
TP-79 Potential Energy and Capacity Gains from Flood Control Storage Reallocation at Existing U.S. Hydropower Reservoirs
TP-80 Use of Non-Sequential Techniques in the Analysis of Power Potential at Storage Projects
TP-81 Data Management Systems of Water Resources Planning
TP-82 The New HEC-1 Flood Hydrograph Package
TP-83 River and Reservoir Systems Water Quality Modeling Capability
TP-84 Generalized Real-Time Flood Control System Model
TP-85 Operation Policy Analysis: Sam Rayburn Reservoir
TP-86 Training the Practitioner: The Hydrologic Engineering Center Program
TP-87 Documentation Needs for Water Resources Models
TP-88 Reservoir System Regulation for Water Quality Control
TP-89 A Software System to Aid in Making Real-Time Water Control Decisions
TP-90 Calibration, Verification and Application of a Two-Dimensional Flow Model
TP-91 HEC Software Development and Support
TP-92 Hydrologic Engineering Center Planning Models
TP-93 Flood Routing Through a Flat, Complex Flood Plain Using a One-Dimensional Unsteady Flow Computer Program
TP-94 Dredged-Material Disposal Management Model
TP-95 Infiltration and Soil Moisture Redistribution in HEC-1
TP-96 The Hydrologic Engineering Center Experience in Nonstructural Planning
TP-97 Prediction of the Effects of a Flood Control Project on a Meandering Stream
TP-98 Evolution in Computer Programs Causes Evolution in Training Needs: The Hydrologic Engineering Center Experience
TP-99 Reservoir System Analysis for Water Quality
TP-100 Probable Maximum Flood Estimation - Eastern United States
TP-101 Use of Computer Program HEC-5 for Water Supply Analysis
TP-102 Role of Calibration in the Application of HEC-6
TP-103 Engineering and Economic Considerations in Formulating
TP-104 Modeling Water Resources Systems for Water Quality
TP-105 Use of a Two-Dimensional Flow Model to Quantify Aquatic Habitat
TP-106 Flood-Runoff Forecasting with HEC-1F
TP-107 Dredged-Material Disposal System Capacity Expansion
TP-108 Role of Small Computers in Two-Dimensional Flow Modeling
TP-109 One-Dimensional Model for Mud Flows
TP-110 Subdivision Froude Number
TP-111 HEC-5Q: System Water Quality Modeling
TP-112 New Developments in HEC Programs for Flood Control
TP-113 Modeling and Managing Water Resource Systems for Water Quality
TP-114 Accuracy of Computer Water Surface Profiles - Executive Summary
TP-115 Application of Spatial-Data Management Techniques in Corps Planning
TP-116 The HEC's Activities in Watershed Modeling
TP-117 HEC-1 and HEC-2 Applications on the Microcomputer
TP-118 Real-Time Snow Simulation Model for the Monongahela River Basin
TP-119 Multi-Purpose, Multi-Reservoir Simulation on a PC
TP-120 Technology Transfer of Corps' Hydrologic Models
TP-121 Development, Calibration and Application of Runoff Forecasting Models for the Allegheny River Basin
TP-122 The Estimation of Rainfall for Flood Forecasting Using Radar and Rain Gage Data
TP-123 Developing and Managing a Comprehensive Reservoir Analysis Model
TP-124 Review of U.S. Army corps of Engineering Involvement With Alluvial Fan Flooding Problems
TP-125 An Integrated Software Package for Flood Damage Analysis
TP-126 The Value and Depreciation of Existing Facilities: The Case of Reservoirs
TP-127 Floodplain-Management Plan Enumeration
TP-128 Two-Dimensional Floodplain Modeling
TP-129 Status and New Capabilities of Computer Program HEC-6: "Scour and Deposition in Rivers and Reservoirs"
TP-130 Estimating Sediment Delivery and Yield on Alluvial Fans
TP-131 Hydrologic Aspects of Flood Warning - Preparedness Programs
TP-132 Twenty-five Years of Developing, Distributing, and Supporting Hydrologic Engineering Computer Programs
TP-133 Predicting Deposition Patterns in Small Basins
TP-134 Annual Extreme Lake Elevations by Total Probability Theorem
TP-135 A Muskingum-Cunge Channel Flow Routing Method for Drainage Networks
TP-136 Prescriptive Reservoir System Analysis Model - Missouri River System Application
TP-137 A Generalized Simulation Model for Reservoir System Analysis
TP-138 The HEC NexGen Software Development Project
TP-139 Issues for Applications Developers
TP-140 HEC-2 Water Surface Profiles Program
TP-141 HEC Models for Urban Hydrologic Analysis

TP-142 Systems Analysis Applications at the Hydrologic Engineering Center
TP-143 Runoff Prediction Uncertainty for Ungauged Agricultural Watersheds
TP-144 Review of GIS Applications in Hydrologic Modeling
TP-145 Application of Rainfall-Runoff Simulation for Flood Forecasting
TP-146 Application of the HEC Prescriptive Reservoir Model in the Columbia River Systems
TP-147 HEC River Analysis System (HEC-RAS)
TP-148 HEC-6: Reservoir Sediment Control Applications
TP-149 The Hydrologic Modeling System (HEC-HMS): Design and Development Issues
TP-150 The HEC Hydrologic Modeling System
TP-151 Bridge Hydraulic Analysis with HEC-RAS
TP-152 Use of Land Surface Erosion Techniques with Stream Channel Sediment Models
TP-153 Risk-Based Analysis for Corps Flood Project Studies - A Status Report
TP-154 Modeling Water-Resource Systems for Water Quality Management
TP-155 Runoff simulation Using Radar Rainfall Data
TP-156 Status of HEC Next Generation Software Development
TP-157 Unsteady Flow Model for Forecasting Missouri and Mississippi Rivers
TP-158 Corps Water Management System (CWMS)
TP-159 Some History and Hydrology of the Panama Canal
TP-160 Application of Risk-Based Analysis to Planning Reservoir and Levee Flood Damage Reduction Systems
TP-161 Corps Water Management System - Capabilities and Implementation Status